Terrain-Aided Navigation of an Unpowered Tactical Missile Using Autopilot-Grade Sensors

W. E. Longenbaker*
Rockwell International, Columbus, Ohio

This paper assesses the feasibility of applying a terrain-aided navigation concept, using nonlinear Kalman filtering techniques, to an unpowered tactical missile. The brief flight time and predictable missile flight path dynamics lead to the definition of a velocity-based strapdown navigation algorithm which utilizes the existing autopilot-grade sensors. The navigation states are corrected by the error estimates of the Kalman filter which uses frequent radar altimeter measurements and terrain slope information (derived from an onboard digitized map) to provide essentially continuous position updating. Covariance analysis and Monte Carlo simulation techniques are applied to predict system performance. Results are obtained which indicate that the accuracy of this weapon/guidance combination may be sufficient to defeat airfields with area munitions.

Introduction

THIS work was initiated in 1981 to study the application of autonomous terrain-aided navigation to the U.S. Air Force GBU-15 weapon. The purpose was to assess the feasibility of applying the Sandia Inertial Terrain-Aided Navigation (SITAN) guidance concept to the GBU-15 weapon system, as an alternative to the existing guidance concept that employs manual target acquisition and an electro-optical seeker for terminal guidance. This combination of the GBU-15 weapon and the SITAN concept was perceived to be a cost-effective solution to the Air Force requirements for an airfield defeat system with all-weather and day/night capabilities.

GBU-15

The GBU-15 missile is currently in production for the U.S. Air Force and is an outgrowth of the original "smart bombs" which were first used in the Vietnam conflict. It is an unpowered vehicle that can be launched below 1000 ft at ranges on the order of 5 miles. It was designed as a modular concept and is composed of a 2000 lb bomb, a control section in the rear, and a television guidance unit on the front end. The control section also includes data link hardware that allows an operator in the launch aircraft to steer the weapon after launch by viewing the video seeker output. Thus it is the role of the "man-in-the-loop" to accomplish the target acquisition function by positioning cross-hairs on the desired target. Tracking can be done either manually by the operator or by switching to the automatic track circuitry in the missile which utilizes an edge (contrast) tracking scheme. The weapon has an analog autopilot and employs either acceleration or attitude control, depending on the mission epoch. The autopilot sensors include a directional/vertical (D/V) gyro, a roll gyro, and two body-mounted accelerometers. All of these sensors are considered to be "autopilot-grade" devices—that is, their requirements were originally specified without any need to perform a navigation function.

Presented as Paper 82-1510 at the AIAA Guidance and Control Conference, San Diego, Calif., Aug. 9-11, 1982; submitted Aug. 9, 1982; revision received May 5, 1983. Copyright © American Institute of Aeronautics and Astronautics, Inc.,1982. All rights reserved.

*Member of Technical Staff, Missile Systems Division. Currently Member of Technical Staff, Bell Telephone Laboratories, Columbus, Ohio.

SITAN

The SITAN guidance approach was conceived by the Sandia Laboratories in the 1974-75 time frame as an alternative to correlation-based terrain-aided navigation schemes (e.g., TERCOM[7]) which had then been receiving great attention by the scientific community. Hostetler[1,2] first described the concept and it was shown that a nearly continuous position-updating scheme might provide greater accuracy than the correlation-based algorithms. Hostetler and Beckmann[3] later reported the results of captive flight testing (fall 1975), in which an inertial navigation system (INS) was successfully updated by the SITAN algorithm. Further flight test results (summer 1976) were reported by Andreas et al.,[4] which reaffirmed the success of the approach and detailed various techniques for linearization of the Kalman filter measurement model. At the 1978 AIAA Guidance and Control Conference, Hostetler[5] extended the concept to include navigation methods other than the INS-based approaches and postulated that the SITAN algorithm could be cost-effective when applied to inexpensive navigation systems.

The SITAN hardware configuration that was flight-tested included an INS, a radar altimeter, and a digital computer (with a digitized terrain map). The guidance philosophy is to use frequent radar altimeter measurements to form what is essentially a continuous position-updating scheme. Downrange and crossrange positions are not directly measured, but it is recognized that variations between expected clearance and actual altimeter clearance measurements are caused by errors in all three position estimates—downrange (x_e), crossrange (y_e), and inertial altitude (h_e). The problem is to determine how each position error is contributing to the clearance error (c_e). If the x and y errors are small enough, then a linear model of the altimeter measurement error is possible, utilizing the terrain slopes in the downrange and crossrange directions. This geometry is shown in Fig. 1.

The slopes can be obtained from the stored terrain map. By processing a sequence of altimeter measurements and comparing the information available at each update, the contributions of x_e, y_e, and h_e to c_e can all be deduced. The more the terrain slopes vary throughout the flight, the richer is the information contained in the sequence of measurements. An extended Kalman filter is the mathematical algorithm that is used to extract these position error estimates.

The guidance concept is basically composed of four parts: a navigation system, a terrain map, a radar altimeter, and the

Kalman filter (see Fig. 2). Based on the current best estimate of position provided by the navigation system, an expected clearance is determined by extracting the local terrain altitude from the map data base. At that point, an altimeter measurement is taken and the error between expected and actual clearance is observed. The Kalman filter algorithm is supplied with estimates of the local terrain slopes (x and y axes) in order to estimate what errors are present in the navigation system. As these errors are identified, the navigation system states are corrected, and after a sequence of these updates, large launch position errors can be gradually reduced enroute to the target.

There are several possible techniques for obtaining the required slope information. One approach is to calculate the local slope at the estimated (x,y) position. However, when large position errors are present (relative to the correlation length of the terrain), then the estimated slope information is virtually useless, and filter divergence is likely to occur. Furthermore, if the slope is estimated from only a few terrain data points, then map modeling noise and quantization errors will produce noisy slope estimates. The preferred approach is to use a larger part of the data base (centered on the estimated position) to obtain well-behaved estimates and to enhance filter convergence properties. There are many ways to do this, as discussed by Hostetler,[5] all emphasizing the accomplishment of the linearization using stochastic weighting criteria. The selected approach for this study is discussed later in this paper.

Since the linearized slope information is the key link between observed clearance errors and downrange and crossrange estimates, the validity of the linearization is essential. By restricting the usage of the system to cases in which the launch error is small as compared to the correlation length of the terrain, the terrain slope estimates are made sufficiently accurate to ensure successful filter convergence. In this respect, SITAN is different from the well-known TERCOM guidance concept, which can successfully converge in spite of very large launch errors. However, the usage of a correlation-based algorithm such as TERCOM was considered to be less suitable for this application, since the relatively inaccurate GBU-15 sensors would not permit a simple correlation algorithm to be derived. Furthermore, as is discussed later in this paper, an extension of the SITAN concept using parallel Kalman filters[9] can be applied to greatly reduce the problems caused by large initial position errors.

GBU-15/SITAN

The subject of this paper is the development of a radically different approach to the current GBU-15 guidance scheme. Its effect on the vehicle configuration would include the addition of a radar altimeter and a digital computer (including a terrain map), the removal of the TV seeker, data link hardware, and analog autopilot, and the expansion of the aircraft interface. In addition, the single bomb would probably be replaced with area munitions, since point accuracy would no longer be attainable. The existing autopilot sensors would be retained, and they would be used to synthesize navigation estimates in a strapdown fashion. Thus, it is conjectured that the relatively crude information obtained from the autopilot sensors would be adequate to perform a navigation function (with the aid of SITAN).

Although the basic goal of the study was to assess the accuracy of the proposed weapon/guidance scheme, it was also desired to focus the study on a realistic operational use. Thus, it was decided to view the concept as a part of a preplanned mission, performing the low altitude delivery of area munitions against airfield targets. The decision was also made to develop the concept with the assumption that the missile would have access to the launch aircraft INS data at weapon launch. The intent was to use SITAN to obtain a terminal position fix, not a global fix.

The technical tasks of the study were organized as follows:

1) Navigation algorithm definition. It was desired to structure an algorithm that would best use the available sensor information in order to form position estimates.

2) Kalman filter formulation. After the algorithm definition was completed, an error analysis would be done to identify the dominant error sources and to model how these errors would propagate through the navigation algorithm. A simplified error dynamics model would be incorporated into the Kalman filter, with a description of the statistical properties of the error sources.

3) Covariance analysis. The first assessment of the system performance would be obtained through this standard technique for evaluation of Kalman filters.

4) Simulation development. If results of the covariance analysis were promising, a complete six-degree-of-freedom (6-DOF) simulation would be developed to provide a more thorough model of the system.

5) Performance evaluation. Execution of the simulation would then provide a Monte Carlo analysis of expected system performance and a determination of the preliminary system requirements.

Navigation Algorithm Development

The function of the navigation algorithm is to estimate position in the local earth coordinate frame (in this case, the local frame is defined at launch and remains unchanged throughout the 1-min flight). Most navigation systems accomplish this function through an inertial navigator platform,

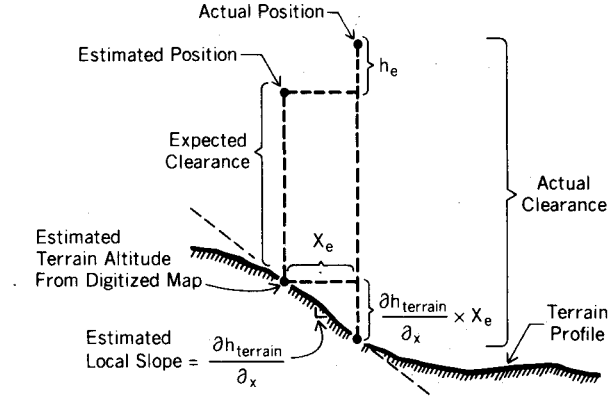

Fig. 1 SITAN measurement geometry

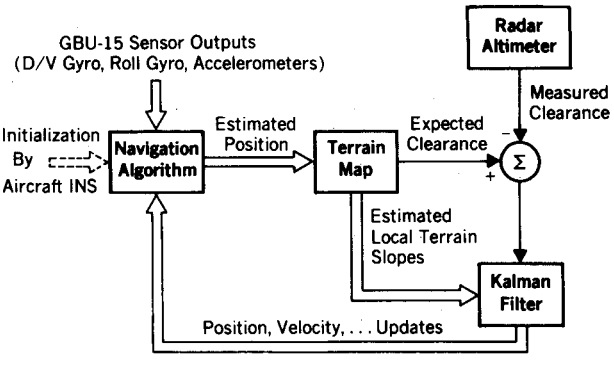

- **GBU-15 data link and EO seeker are removed**
- **Aircraft interface is expanded**
- **Radar altimeter, digital processor, and memory are added**

Fig. 2 GBU-15/SITAN guidance concept.

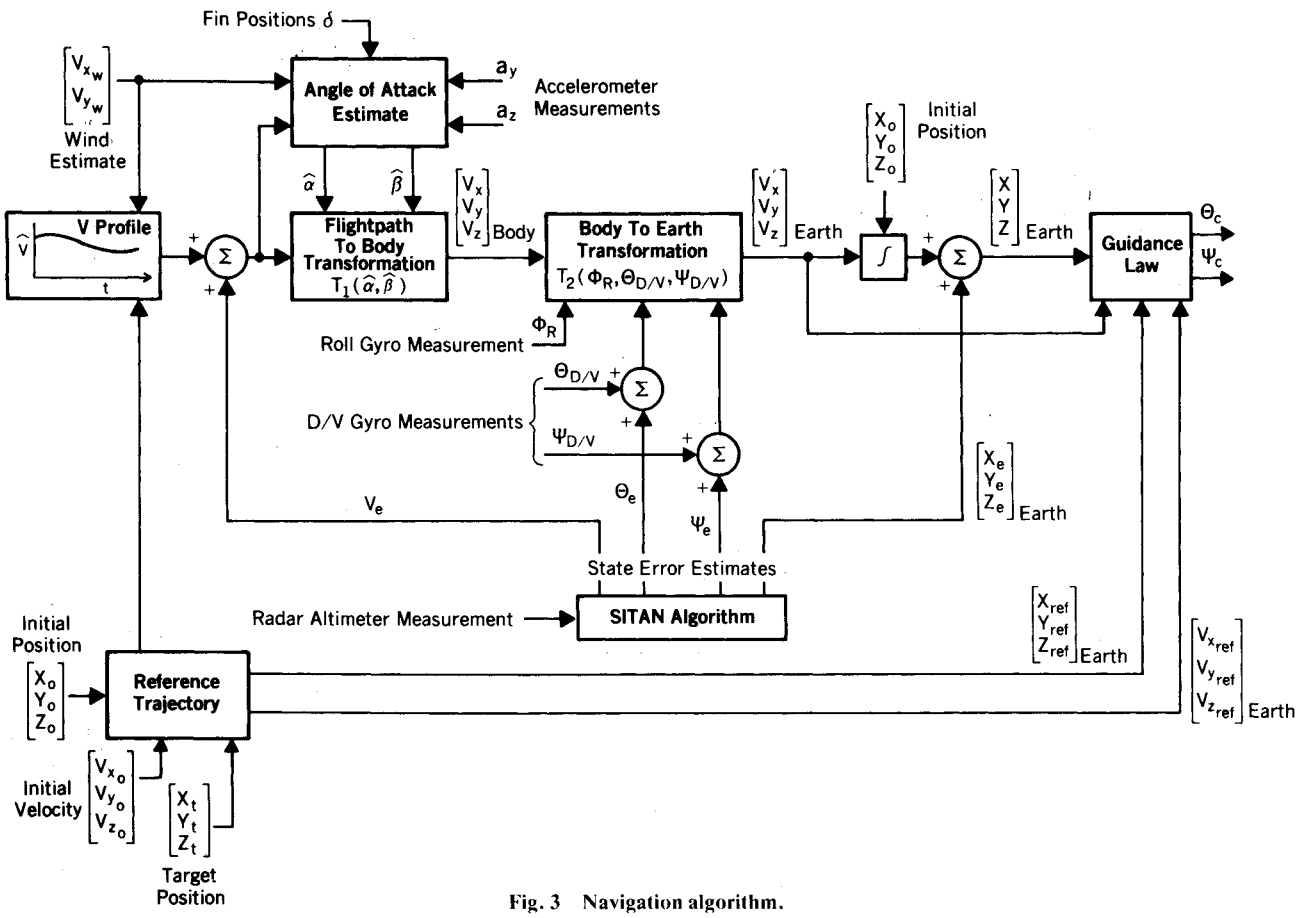

Fig. 3 Navigation algorithm.

a strapdown system, or a combination of the two. These are acceleration-based systems; that is, they form an estimate of inertial (or local earth) acceleration and then double-integrate to obtain position estimates. This is the best method for navigation when highly accurate sensors are available and the flight time is long between position updates. Variations in acceleration due to missile thrusting, aerodynamic uncertainty, and wind gust effects make it essential to measure acceleration.

The unique attributes of the proposed GBU-15/SITAN system make it attractive to consider a departure from the standard approach. The GBU-15 is basically a very heavy unpowered bomb. Its flight path dynamics are very predictable, and it is relatively insensitive to wind gusts. For these reasons, and since flight time is only about 1 min, it is reasonable to consider a velocity-based navigation system. In this way, angular errors of the GBU-15 gyroscopes will propagate into position errors as a linear function of time (t), instead of the t^2 effect that occurs in an acceleration-based system. In addition, this approach makes the navigation system less dependent on the accuracy of the accelerometers, which are of a poorer quality than the D/V gyro. Furthermore, the small acceleration errors that do occur will not become excessive in so short a flight, and their effect is negated by the nearly continuous (e.g., every 200 ft) pseudo-position update of the SITAN concept.

Since the GBU-15 weapon does not possess any type of velocity sensor, it is necessary to have a precomputed estimate of the vehicle's expected velocity time history. This requires knowledge of the planned launch velocity as well as the nominal trajectory enroute to the target. These requirements may seem overly restrictive; however, the information should be readily available and entirely consistent with the preplanned mission concept. Since there will be small course corrections as position and velocity errors are identified by the SITAN algorithm, the velocity history is not predetermined for each position axis, but rather, only the overall magnitude is specified. This magnitude will vary depending on the correction, but should remain close enough to the nominal value for the purposes of the algorithm.

Figure 3 shows the form of the navigation algorithm. The velocity profile is precomputed according to the trajectory that will be flown. The trajectory is a function of launch range, velocity, and heading. (Recall that the aircraft provides an initialization of position, velocity, and attitude at launch; or else, the pilot strives to achieve the desired launch states.) The nominal trajectory will feature a level or lofted launch, 0.5- to 1-g pullup and pitchover maneuvers, a relatively long glide epoch, then a terminal maneuver which would be dependent on the type of area munitions that are used. The velocity magnitude is transformed to the flight path (wind) coordinate system by using estimates of angle of attack (α) and sideslip angle (β). These estimates are obtained by processing accelerometer measurements (y and z axes), and through knowledge of velocity as well as the highly predictable aerodynamics of the vehicle. Thus trim angles of attack are related to normal forces, which are related to the accelerometer measurements. Both the α and β estimates are modified to reflect steady-state wind effects.

It is interesting to note that deviations in normal acceleration because of wind gusts and course corrections will produce corresponding changes in the α and β estimates. Therefore, the navigation algorithm is not oblivious to the two available acceleration measurements. Although there still is no way to estimate changes in axial acceleration, this error source has a minimal effect and will be considered in the Kalman filter model.

Next, the velocity vector is transformed from body axes to local Earth axes using the angle measurements of the D/V gyro and the roll gyro. (For this application, the erection circuit of the D/V gyro would be disabled.) The initialization of these gyros is accomplished either by using the aircraft INS

Table 1 System error sources

Error source		Values (1σ)	Type
Initial position	$-X$	500 ft	Bias
	$-Y$	500 ft	Bias
	$-Z$	100 ft	Bias
Initial velocity magnitude		5.6 ft/s	Bias
Initial attitude	$-\phi$	0.25 deg	Bias
	$-\theta$	0.25 deg	Bias
	$-\psi$	0.25 deg	Bias
Accelerometer	$-Y$	5 mg	Bias
	$-Z$	5 mg	Bias
D/V gyro uncage and pickoff	$-\theta$	0.36 deg	Bias
	$-\psi$	0.36 deg	Bias
D/V gyro pickoff	$-\theta$	0.02 deg	Noise
	$-\psi$	0.02 deg	Noise
D/V gyro drift	$-\theta$	0.002 deg/s	Bias
	$-\psi$	0.003 deg/s	Bias
D/V gyro drift	$-\theta$	0.0033 deg/s	Noise
	$-\psi$	0.0055 deg/s	Noise
Roll gyro uncage and pickoff	$-\psi$	0.36 deg	Bias
	$-\phi$	0.36 deg	Bias
Roll gyro pickoff	$-\psi$	0.04 deg	Noise
	$-\phi$	0.04 deg	Noise
Roll gyro drift	$-\psi$	0.002 deg/s	Bias
	$-\phi$	0.003 deg/s	Bias
Roll gyro drift	$-\psi$	0.0033deg/s	Noise
	$-\phi$	0.0055 deg/s	Noise
Altimeter/map		5-10 ft	Noise

or simply by assuming prelaunch values. It is stressed that no complicated transfer alignment is required with this type of guidance scheme. Furthermore, the very short flight permits the navigation to be performed under a flat earth assumption.

The estimate of velocity in the local earth coordinate system is integrated to obtain position estimates. As discussed in the Introduction and again in the next section, the Kalman filter is then used to update the position estimates as well as the velocity profile, heading and pitch angle. The attitude control loops of the vehicle are commanded to steer the weapon onto the desired trajectory. Yaw (ψ) is commanded to achieve the desired heading (probably just pointing at the target), whereas pitch (θ) is commanded to follow the predetermined vertical plane trajectory. This nominal trajectory is defined by a table look-up of the desired altitude and altitude rate as a function of range and range rate. If large course corrections are made, a slight adjustment of the velocity profile can also be made to reflect the deceleration caused by a large α or β.

There are several improvements and/or changes to the navigation algorithm to be considered. Portions of the algorithm are as yet undefined, including the reference trajectory computation and the regulator control law for course corrections. In addition, the computational errors associated with finite precision arithmetic have not been assessed. Finally, it is expected that the α and β estimates can be improved by simple low pass filtering. This will be especially beneficial to diminish the effects of high frequency wind gusts.

Kalman Filter Formulation

After the navigation algorithm was defined, it was necessary to conduct an error analysis of the algorithm. The system error sources are given in Table 1. The initial position, velocity and attitude errors imply that a handoff from the aircraft INS is accomplished. These error levels are consistent with the quality expected from a crude aircraft position fix shortly before weapon launch. Aerodynamic uncertainty has not been included, but its effects are secondary and will be assessed during the covariance analysis studies. Also, scale factor errors and g-sensitive errors are not listed since the short flight and relatively smooth trajectory make their effects negligible. The standard error analysis technique using sensitivity coefficients was applied, and the analysis was simplified by assuming that the dominant error sources are either angular errors or the velocity error.

The results of the analysis are shown in Fig. 4. By assuming that α, β, ψ, and ϕ are small angles, and by neglecting roll error (it only makes a small contribution to ΔV_{ye}), then the equations from Fig. 4a can be approximated by those from Fig. 4b. For this analysis, the following definitions apply:

$$\psi=\psi_{D/V},\quad \theta=\theta_{D/V},\quad \epsilon_y=\psi_{D/V}-\beta,\quad \epsilon_z=\theta_{D/V}+\alpha$$

$$\phi=\tan^{-1}\left(\frac{-\cos\psi_{D/V}\tan\theta_{D/V}}{\sin\psi_{D/V}\sin\theta_{D/V}\tan\phi_{roll}-\cos\theta_{D/V}}\right)$$

where ϕ, θ, and ψ are consistent with a ϕ-θ-ψ Euler angle definition.

Note that the simplified model does not distinguish between θ and α errors, nor between ψ and β errors. The result is a six-state error propagation model (velocity magnitude, elevation, azimuth and three positions) which can be used as the dynamics model in a suboptimal Kalman filter. If significant lateral excursions are desired so that ψ changes considerably, then the model can be modified accordingly. Also, it may be desirable to include roll error as a state if an attitude initialization from the aircraft INS is not available. The Kalman filter dynamics model was completed by specifying the assumed statistics of the error sources. These statistics were conservatively defined, introducing fictitious noise levels to offset the effects of unmodeled dynamics (e.g., angular drift errors and axial acceleration errors) and nonlinearities. Although the primary motivation for the usage of only six states was to minimize the model complexity and computational burden, it is also true that the unmodeled drift and acceleration biases are less identifiable in so brief a flight, especially when no transfer alignment is done. Therefore, it was expected at the onset that six filter states would prove to be adequate for the dynamics model.

The Kalman filter measurement model was previously identified in Fig. 1. The measurement error is modeled as white noise, and represents the errors in the altimeter measurement as well as inherent map errors. Although the altimeter measurement error is never truly uncorrelated, the white noise approximation is most valid when 1) the vehicle altitude is low; 2) the updates are slow as compared to the terrain correlation length; 3) the terrain signature is not very rough; and 4) the antenna beamwidth is narrow. As will be discussed later in this paper, the validity of the approximation can also be jeopardized by the terrain slope linearization when very large position errors are present.

It is expected that the digital processor requirements for implementation of all the guidance functions would be minimal. It is estimated that the navigation algorithm would absorb 20% of the computational time of the Zilog Z-8000 processor (6-MHz clock) using an 8-Hz cycle time. The Kalman filter should require 15% of the available time at a 4-Hz rate, while the remaining attitude control loop command generation and shaping filters would require 20% at a 250-Hz rate. Thus, the processor is expected to be about 55% loaded. Total memory requirements are modest except for the sizeable digital map requirements (50 to 100 K bytes). All Kalman filter calculations would be made "on-line" (real-time), since most of the matrix calculations are dependent on the real-time clearance measurements.

Covariance Analysis

Once the suboptimal Kalman filter model was specified, it was desirable to predict how much the algorithm could reduce the launch point CEP. Ordinarily, the steady-state value of

$$\begin{bmatrix}\Delta V_{x_e}\\ \Delta V_{y_e}\\ \Delta V_{z_e}\end{bmatrix} = \left[\begin{array}{c|c|c|c|c|c} -V[(\psi-\beta)\cos\theta+\alpha] & -V\sin\theta & 0 & -V(\psi+\alpha\cos\theta) & V(\psi-\beta)\cos\theta & \cos\theta \\ \hline -V\cos\theta & -V\phi\cos\theta & -V(\alpha\cos\theta+\sin\theta) & -V\phi\cos\theta & V & -\phi\sin\theta-(\psi-\beta) \\ \hline -V[(\psi-\beta)\sin\theta+\phi] & -V[\alpha\sin\theta-\cos\theta] & -V[\phi\sin\theta+(\psi-\beta)] & -V[\alpha\sin\theta-\cos\theta] & V[\phi+(\psi-\beta)\sin\theta] & \alpha\cos\theta+\sin\theta \end{array}\right] \times \begin{bmatrix}\Delta\psi\\ \Delta\theta\\ \Delta\phi\\ \Delta\alpha\\ \Delta\beta\\ \Delta V\end{bmatrix}$$

a)

$$\begin{bmatrix}\Delta V_{x_e}\\ \Delta V_{y_e}\\ \Delta V_{z_e}\end{bmatrix} = \left[\begin{array}{c|c|c} \cos\theta_{D/V} & 0 & -V\sin\theta_{D/V} \\ \hline 0 & -V\cos\theta_{D/V} & 0 \\ \hline \sin\theta_{D/V} & 0 & V\cos\theta_{D/V} \end{array}\right] \times \begin{bmatrix}\Delta V\\ \Delta\varepsilon_y\\ \Delta\varepsilon_z\end{bmatrix}$$

b)

Fig. 4 Error propagation modeling.

the filter's covariance matrix would be calculated for this purpose. However, a complete covariance analysis was necessary in this case for two reasons: 1) the filter was known to be suboptimal (six states), hence its own covariance estimate would be erroneous; and 2) there exists no true steady state in the SITAN concept since the algorithm only works when there is a continuous variation in the magnitude of the local terrain slopes.

The computer program that was used to do the covariance analysis is called SAMUS,[6] and was developed by Rockwell in 1970 and modified for this application. The suboptimal filter performance was evaluated vs a 10-state "truth" model (the six filter states, plus aerodynamic drag uncertainty, yaw drift, pitch drift, and an x-axis wind gust state) and assuming a straight and level flight path. Quasi-steady-state results were obtained by randomly generating terrain slope information (Gauss-Markov process) and then averaging the states over an interval of time. CEP was computed from the downrange and crossrange position errors, and evaluated as a function of the standard deviation of the random terrain slopes (σ_s). In addition, the results were obtained parametrically with respect to the standard deviation of the measurement noise (σ_M).

It is important to note that this covariance analysis approach implicitly assumes that the filter has access to true slope information, even though that is impossible when large position errors are present. Consequently the utility of the covariance analysis was only to evaluate quasi-steady-state errors, in which case the estimated slopes would be nearly equal to the true slopes (since the position errors would be small). Since the covariance analysis would not properly assess filter convergence, it remained to construct a simulation for that purpose.

The results of the covariance analysis are shown in Fig. 5. It is expected that the region of operation using an available off-the-shelf altimeter model (e.g., Honeywell APN-194) would be between the two curves shown in the figure. The results are representative of terrain in which the slopes have a 600-m correlation length, and are consistent with a vehicle flight time of 50 s. (The GBU-15 will have flown approximately 5 miles at that point.) Note that navigation CEP has been evaluated, and not "holes in the ground."

Although the six-state error propagation model did not estimate the attitude drift biases, the neglect of these errors did not significantly degrade results. However, the unmodeled aerodynamic drag bias and axial wind gust effects did produce harmful effects on the velocity and downrange estimates. Consequently the filter process noise statistics were increased to offset the effects of the unmodeled dynamics. Although the validity of this crude sensor modeling was of fundamental importance, it was seen that the modeled measurement noise

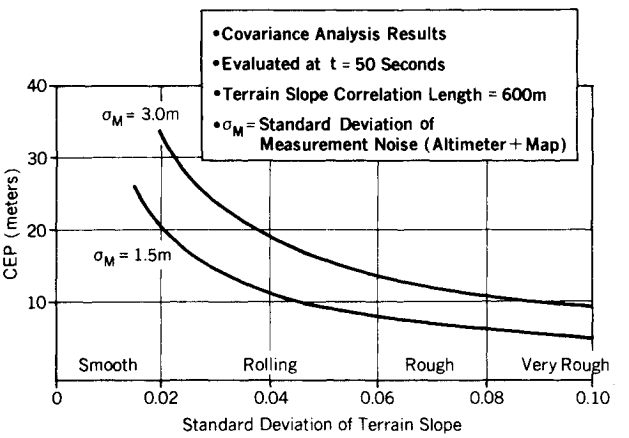

Fig. 5 Results of covariance analysis.

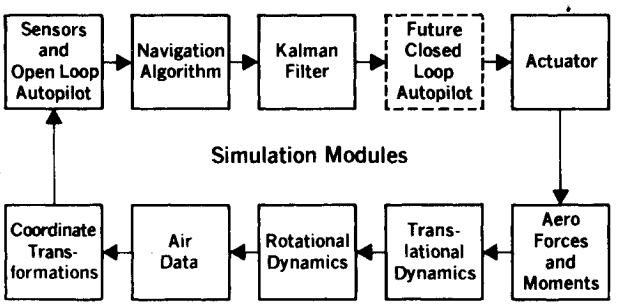

Fig. 6 Structure of six-degree-of-freedom simulation.

(altimeter and map errors) was still a more significant error source than the gyro and accelerometer errors. Based on these results, the GBU-15/SITAN concept appeared to be promising, and it remained to confirm through simulation that the filter would converge and attain these predicted results.

Simulation Development

The simulation was intended to assess those effects that could not be studied via the covariance analysis technique: How should the terrain slopes be estimated? How do slope estimation errors affect algorithm convergence? How fast will the filter converge? Is the filter model adequate? How does it perform using real terrain models?

The structure of the simulation is shown in Fig. 6. It was developed from the basic GBU-15 nonlinear six-degree-of-

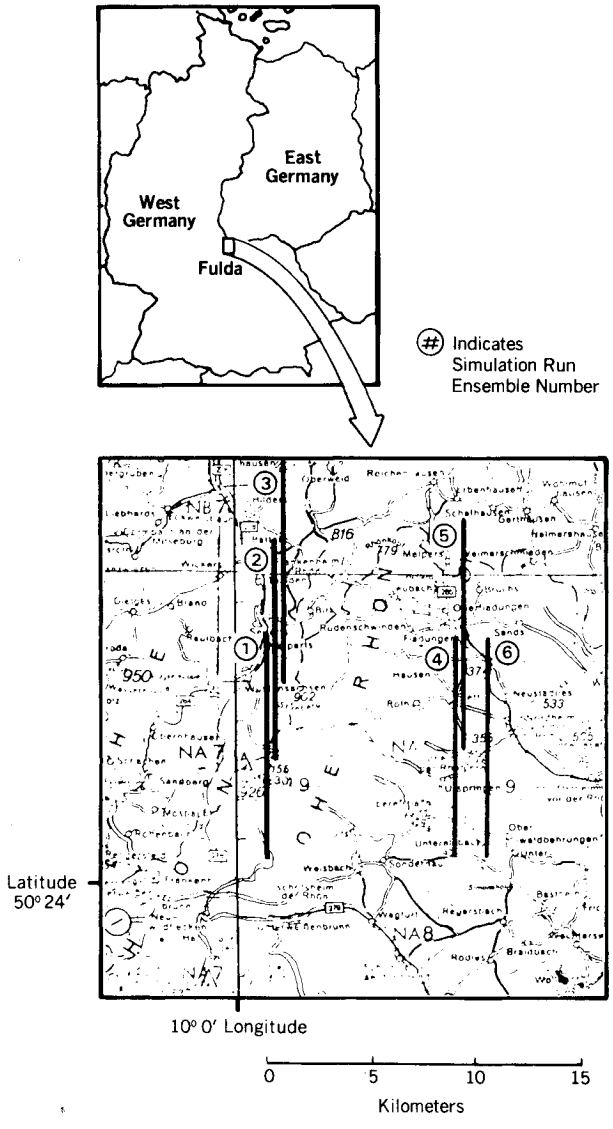

Fig. 7 Location of digitized terrain map.

freedom simulation, but required significant changes to model the navigation algorithm, Kalman filter, and digitized terrain map. Since the important task was to evaluate state estimation errors, no attempt was made to track a reference trajectory (although that would be required operationally). Instead, a simple canned trajectory was flown (open-loop commands) during simulation execution. Naturally, the flat earth assumption was also used in the simulation. All error sources (Table 1) were included in the simulation either as random noise or part of random Monte Carlo initializations.

To increase confidence in the simulation predictions, specific digitized data were obtained from the Defense Mapping Agency representing the terrain surface near the Fulda region of West Germany. Figure 7 shows the location of this terrain, and also indicates the various paths that were overflown (south to north), using the simulation. The use of several terrain segments allowed the filter convergence to be assessed for varying degrees of terrain roughness. By entering the map data base with the estimated position coordinates, the estimated clearance was obtained. Similarly, the true clearance was computed through knowledge of the true position coordinates.

As explained earlier, the terrain map is also used to provide estimates of the local terrain slopes in the downrange and crossrange directions. Since it is recognized that significant position errors can occur which could introduce large errors in the slope estimates, a stochastic linearization of the terrain

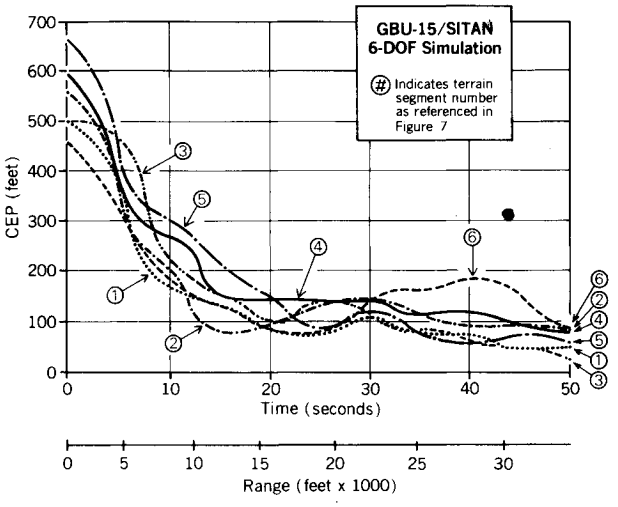

Fig. 8 Monte Carlo simulation results.

surface is performed. This is accomplished by fitting a plane to the nonlinear terrain surface, using a uniformly weighted least squares criterion. The fit area is equal to the $\pm 3\sigma$ errors as estimated by the filter covariance matrix and is centered about the estimated position. In this way, low frequency information describing the general "lay of the land" is obtained. Then, as the position errors are reduced and a smaller fit area is used, the more informative, high frequency terrain undulations are utilized. The great value of this linearization is that the probability of filter convergence is greatly enhanced, although convergence time is increased.

Due to the highly nonlinear nature of the measurement function, the possibility of filter divergence is a serious issue. When divergence occurs, it basically means that the increasing state uncertainties caused by sensor errors have overcome the ability of the altimeter measurements to reduce the errors. Though this latter ability is dependent on the level of altimeter and map noise, it is also strongly influenced by the size of the initial position error and the characteristics of the specific terrain signature. Therefore, an explicit guideline of the GBU-15/SITAN approach is that the weapon system should only be utilized when the expected initial position error lies within acceptable limits for the selected target area.

Another important consideration for this guidance concept is recognition that the linearization process introduces additional measurement error. Consequently the variance of the fit is added to the modeled altimeter/map white noise variance in order to prevent the filter from being overly optimistic about the quality of the measurements (similar to second-order filters). Thus, the system is "open-loop adaptive," in the sense that it adjusts the parameters of its model according to the terrain being overflown and the size of its estimated position errors. It is not "closed-loop adaptive," since the Kalman filter model is not adjusted as a function of the innovation sequence. This "modified" stochastic linearization is discussed in detail in Ref. 5.

The measurement noise caused by the terrain linearization fit error is not truly white, and Hostetler and Beckmann[8] have shown that by modeling this fit noise as a correlated process, superior performance can be achieved. This is especially true when the size of the fit area is on the same order as the terrain overflown between updates. This improvement was not included in this study.

The most important error source that is modeled in the simulation is the altimeter/map measurement noise. It is modeled as 5 ft of white noise plus the effects of the "shortest return." (Conversely, the Kalman filter assumes 10 ft of white measurement noise.) This is a simplified radar altimeter model and represents an attempt to model the actual effect in which the radar altimeter measurement becomes correlated with the terrain profile. The clearance measurement is

Table 2 Actual CEP vs Kalman filter estimate (evaluated at t = 50 s)

Terrain segment no.	CEP, ft, based on actual simulation results	CEP, ft, based on Kalman filter 1σ estimates	Δ, ft (actual-Kalman filter)
③	27	37	−10
①	50	50	0
⑤	60	49	11
④	76	108	−32
②	84	71	13
⑥	88	77	11

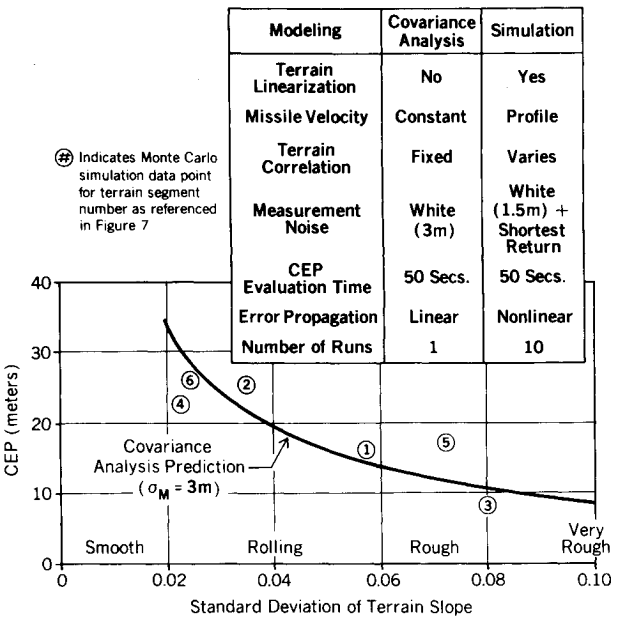

Fig. 9 Simulation results vs covariance analysis prediction.

determined by the shortest distance to the terrain map surface, within the specified altimeter beamwidth. It is assumed that the radar altimeter beam is directed in the estimated "down" direction for the purpose of this analysis. In reality, the shortest return is not the range that the altimeter would measure since pulse returns are integrated and processed in a more sophisticated manner. The study assumed a narrow beamwidth (5 deg), in part to offset the excessively harsh effects of the "shortest return" modeling. Future work would incorporate more complex models for the altimeter/antenna hardware.

Performance Evaluation

The simulation was executed so that the vehicle overflew the six different terrain segments (nominal 0.9 Mach launch speed) that were previously identified in Fig. 7. Ten Monte Carlo initializations were conducted for each segment using all the error sources that were listed in Table 1. Then the CEP for each segment was plotted as a function of time and downrange. This is shown in Fig. 8. The initial position error was intended to be 500 ft (1σ) in x and y, which would result in an initial CEP of 589 ft (assuming a bivariate Gaussian distribution). The variation from the value occurred because only ten Monte Carlo draws were made. Still, the initial CEP was always within ±20% of the intended value. The convergence of the CEP suggests an exponential type of curve, with a time constant equal to about 12 s (10,000 ft). After 50 s of flight, the CEP values ranged from a low of 27 ft to a high of 88 ft. The run set that produced the maximum CEP was subjected to a stretch of terrain late in the flight in which the terrain signature was very poor (σ_s was approximately 0.01), as evidenced by the excursion of the CEP curve well above the 100-ft level. Nevertheless, it was felt that the success of the design was verified by these results.

Monte Carlo simulation executions with higher initial position errors (σ = 850 ft) were also performed for terrain segment 1, and always resulted in filter convergence. Furthermore, the increase in CEP after 40 to 50 s of flight was typically only about 10%. In general, it was found that divergence would not occur for these specific terrain segments until the initial position biases were on the order of 2500 ft.

While the simulation results suggested that the Kalman filter was working correctly, it was still worthwhile to examine the filter performance in detail. In particular, a good criterion by which to assess a filter design is whether the state errors predicted by the filter covariance matrix were somewhat in agreement with the actual errors. Indeed, the examination revealed that in only 5% of the cases did the actual position error ever exceed the bounds of the ±3σ band as defined by the filter covariance matrix. Since the system is highly nonlinear, occurrence of these 3σ "violations" was not unexpected, although filter modeling improvements (such as a correlated measurement model) should reduce or eliminate the problem entirely. Table 2 compares the actual CEP at t = 50 s for each terrain segment vs the CEP as predicted by the Kalman filter (again assuming a bivariate Gaussian distribution). Considering the limited number of simulation runs, the agreement is judged to be good.

To be able to relate these specific segments to other real-world terrain, and also to compare the simulation results vs the covariance analysis predictions, it was necessary to quantify the terrain properties using statistics. Since terrain is not truly a stationary process (hence not ergodic), it is somewhat difficult to compare real terrain statistics with the statistics of stationary random processes (as used in the covariance analyses). Nevertheless, the standard deviation of each terrain segment was evaluated during the last mile of flight, the crossrange and downrange values were averaged, and then the CEP for the particular terrain segment was plotted against these average values.

The results of this procedure are shown in Fig. 9 in which the CEP computations are overlayed on the previous covariance analysis predictions. The results show good agreement, although there are variations caused by many factors: the inability to appropriately quantify terrain statistics; the variation in terrain correlation length from segment to segment, and within each segment; the limited number of Monte Carlo runs (ten); and the varying effect of the "shortest return" altimeter model which introduces more noise as the terrain gets rougher.

Since the performance evaluation is entirely dependent on the validity of the error source models that were used in the simulation, several final comments are appropriate in this respect. The error sources listed in Table 1 include initialization errors that are consistent with a handoff from the launch aircraft INS. If this information is not available, then the pilot must strive to reach predetermined launch states. The initialization errors would certainly increase, and would produce an accompanying degradation in the navigation CEP. Certain approaches can mitigate the harmful effects, such as the usage of a correlated measurement model, the addition of more filter states, or even a parallel Kalman filtering technique,[9] in which the individual filters are initialized with different estimated positions. In the latter approach, the "correct" filter is selected by monitoring the innovation sequence. Sandia Laboratories has shown that extremely good performance can be achieved with this method, effectively eliminating the filter divergence problems associated with large launch position errors. The multiple filter concept permits the retention of the white noise measurement model and is considered to be superior to the usage of a single filter with a correlated measurement model.

Improvements in the altimeter/antenna modeling would also impact the expected accuracy, and are undoubtedly the most important priority for future analyses. Wind gusts and aerodynamic drag uncertainty were also not included in the basic performance evaluation. However, separate Monte Carlo analysis showed negligible increases in CEP due to these errors. Although the angle of attack and sideslip estimators were adversely affected by wind gusts, it is felt that simple low pass filtering would eliminate any problems. In addition, wind shear (steady-state winds as a function of altitude) effects have yet to be investigated. Wind shear would hurt accuracy, but it is not expected to be serious since the vehicle would not be undergoing large altitude excursions.

Conclusions

It has been shown that terrain-aided navigation techniques such as SITAN are feasible approaches to perform the terminal guidance function of short-range tactical weapons when point accuracy is not required. In the specific case of the GBU-15 missile, it has been shown that this function can be accomplished with the existing autopilot-grade sensors and using a velocity-based navigation algorithm. Simulation of the brief weapon flights has shown that a CEP on the order of 75 ft is feasible. The potential accuracy of this approach indicates that further investigation of the concept as an airfield defeat system may be warranted.

Acknowledgments

The author would like to thank Dr. P. R. Hinrichs, Dr. T. C. Sheives, Mr. J. R. Brewer, Mr. R. D. Ehrich, and Mr. R. I. Emmert for their suggestions and contributions to this effort.

References

[1]Hostetler, L. D., "An Analysis of a Terrain-Aided Inertial Navigation System," Sandia Laboratories, Albuquerque, N.M., SAND75-0299, Sept. 1975.

[2]Hostetler, L. D., "A Kalman Approach to Continuous Aiding of Inertial Navigation Systems Using Terrain Signatures," *IEEE Milwaukee Symposium on Automatic Computation and Control Proceedings*, April 1976, pp. 305-309.

[3]Hostetler, L. D. and Beckmann, R. C., "The Sandia Inertial Terrain-Aided Navigation System," Sandia Laboratories, Albuquerque, N.M., SAND77-0521, Sept. 1977.

[4]Andreas, R. D., Hostetler, L. D., and Beckmann, R. C., "Continuous Kalman Updating of Inertial Navigation System Using Terrain Measurements," *National Aerospace and Electronics Conference Proceedings*, May 1978, pp. 1263-1270.

[5]Hostetler, L. D., "Optimal Terrain-Aided Navigation Systems," *AIAA Guidance and Control Conference*, Palo Alto, Calif., Aug. 1978 and Sandia Laboratories, Albuquerque, N.M., SAND78-0874, June 1978.

[6]Osborn, R. F. and Atkinson, M. W., "SAMUS—A Program for State-Space Analysis of Multisensor Systems," Rockwell International, Columbus, Ohio, T70-428/201, April 1970.

[7]Baker, W. R. and Clem, R. W., "Terrain Contour Matching (TERCOM) Primer," Aeronautical System Division, Wright-Patterson AFB, Ohio, ASP-TR-77-61, Aug. 1977.

[8]Hostetler, L. D. and Beckmann, R. C., "Expanding the Region of Convergence for SITAN Through Improved Modelling of Terrain Nonlinearities," *National Aerospace and Electronics Conference Proceedings*, May 1979, pp. 1023-1030.

[9]Sheives, T. C. and Andreas, R. D., "An Alternate Approach for Terrain-Aided Navigation Using Parallel Extended Kalman Filters," Sandia Laboratories, Albuquerque, N.M., SAND79-2198, Dec. 1979.

From the AIAA Progress in Astronautics and Aeronautics Series . . .

REMOTE SENSING OF EARTH FROM SPACE: ROLE OF "SMART SENSORS"—v. 67

Edited by Roger A. Breckenridge, NASA Langley Research Center

The technology of remote sensing of Earth from orbiting spacecraft has advanced rapidly from the time two decades ago when the first Earth satellites returned simple radio transmissions and simple photographic information to Earth receivers. The advance has been largely the result of greatly improved detection sensitivity, signal discrimination, and response time of the sensors, as well as the introduction of new and diverse sensors for different physical and chemical functions. But the systems for such remote sensing have until now remained essentially unaltered: raw signals are radioed to ground receivers where the electrical quantities are recorded, converted, zero-adjusted, computed, and tabulated by specially designed electronic apparatus and large main-frame computers. The recent emergence of efficient detector arrays, microprocessors, integrated electronics, and specialized computer circuitry has sparked a revolution in sensor system technology, the so-called smart sensor. By incorporating many or all of the processing functions within the sensor device itself, a smart sensor can, with greater versatility, extract much more useful information from the received physical signals than a simple sensor, and it can handle a much larger volume of data. Smart sensor systems are expected to find application for remote data collection not only in spacecraft but in terrestrial systems as well, in order to circumvent the cumbersome methods associated with limited on-site sensing.

505 pp., 6×9, illus., $22.00 Mem., $42.50 List

TO ORDER WRITE: Publications Order Dept., AIAA, 1633 Broadway, New York, N.Y. 10019